Rotational motion of dusty structures in glow discharge in longitudinal magnetic field

V. Yu Karasev,* E. S. Dzlieva, A. Yu. Ivanov, and A. I. Eikhvald
Institute of Physics, St. Petersburg State University, Ulyanovskaya st. 1, Peterhof, St. Petersburg, 198504 Russia
(Received 14 August 2006; published 29 December 2006)

The investigation of dust structure formed in glow discharge in an external longitudinal magnetic field with induction up to 400 G applied is presented in this work. The dust structure starts to rotate in the magnetic field. The angular-velocity magnitude is one to two orders larger than one in other discharge types. Its dependence on the magnetic field is nonmonotonic. The rotation direction inverses with an increase of the magnetic induction value up to a certain magnitude B_0. In close range of induction around B_0 and under certain conditions the rotation of the upper and lower parts of the structure in the opposite direction is observed. Rotation is caused by the ion-drag force. The inversion of rotation direction relates with the change of plasma flows in the area of their formation in stratum with the magnetic field applied. The effect of ion flows was investigated in two additional experiments on the observation of structure rotation onset and on gravity-driven probing of stratum. The angular-velocity unhomogeniety allowed us to investigate shearing and to observe melting of the dust crystal. The correlation functions approach showed the occurrence of structure transformation and its phase transition of the meltinglike type in the magnetic field.

DOI: 10.1103/PhysRevE.74.066403 PACS number(s): 52.27.Lw

I. INTRODUCTION

Due to its unique properties, dusty (complex) plasma [1–7] has been an object of advanced research for the last decade. Self-organization in a dust component leads to the formation of a quasicrystalline state with a submillimeter-lattice period of a plasma crystal. On this scale the processes of crystal formation, phase transitions, and polymorphic modifications can be investigated by direct optical observations. It is also possible to measure the energetic distribution of particles and to verify the statements of molecular-kinetic theory directly. Applications of dusty-plasma physics span from space physics [1] to technological processes [2].

The influence of an external drive makes dynamics more complex, so the response on such a drive is an important source of information about the properties of complex systems. For dusty plasma the use of an external magnetic field proved itself as an effective and informative method.

In a majority of cases, the magnetic field acts at granules indirectly in laboratory dusty plasmas. It influences due to flows of electrons and ions to the granules. Electrons and ions first obtain an impulse in the magnetic field and then transfer it to the granules. As a result the mechanical state of the plasma dusty component may change. Firstly, the magnitude and direction of the angular velocity of single-granules spinning (macrospin) changes [8–11]. Secondly, dust structures start to rotate as a whole [11–15].

The rotation of dusty structures in the magnetic field was discovered in the discharge chamber of special construction SPLE [16]. Investigations in rf discharge were held in Ref. [12], where the magnetic-field induction was invariable. The interpretation of the dust structures rotation motion in the magnetic field is suggested in Refs. [12,17]. The origin of rotation motion is the action of the ion drag force (the impulse obtained by ions in the magnetic field and transferred to granules in the collisions) [18]. The electron drag force is probably always essentially less [3,18]. This fact was checked experimentally in conditions of ECR plasma [19]. Some properties of the rotation motion mechanism are not clear up to now. The most important of them are (i) the dependence of the rotation angular velocity on the number of particles in the structure [12,20] or in the cluster [14]; (ii) reasons of rotation inversion; (iii) the area of formation of plasma flows to the structure [21–24]; (vi) the specificity of conditions in discharge chambers of different construction; and (v) an effect of neutral drag [13,25]. Controlling the flows by the means of the magnetic field may change the energy-release distribution, parameters of diffusion, and energy transition in the discharge chamber [26,27]. This way both the mechanical state of the dusty component and the ordering of the dusty structure may be changed. For example, it is possible to melt or crystallize the dust structure, to change the dust crystal lattice, and to perform plastic and elastic deformations.

The electrons that define the properties of glow discharge plasma are effectively influenced by the magnetic field of several hundreds of gausses. Therefore the magnetic field of this magnitude was used in conducted experiments. In this paper we present the results of the dust structures state and the behavior investigations held in conditions of dc glow discharge with an external magnetic field applied.

Section III conserns basic experimental results, one of which is the inversion of rotation that occurred with a variation of the magnetic field only. Section IV contains an interpretation of these results. Besides the numerical estimations, the interpretation also required two additional experiments. In Sec. V the correlation functions approach was applied to study the dusty-structure internal-states variation.

II. EXPERIMENTAL SETUP

In our experiments a dusty plasma is formed in the head (glowing) part of a stratum [28] and near diaphragm (nar-

*Electronic address: viktor.karasev@pobox.spbu.ru

rowed part of discharge tube). The experimental setup had several modifications; in general it is presented in Fig. 1(a). The discharge tube had a vertical orientation with the cathode downward. It was placed inside the magnetic coils. The containers with different powders assigned for injection to the discharge were situated at the top of the tube above the anode. An oil-free vacuum system was used for pumping out and filling with gases. In the case of spectrally pure gases usage, the discharge tube had been trained for a necessary time by an increased discharge current. In experiments the power supply of discharge was stabilized. In order to define deviations in the parameters of plasma-forming gases the current-voltage diagrams were measured before and after each observation.

Magnetic coils were coaxial to the discharge tube. In order to perform visual observations, coils were moved apart for 9 cm. The spatial distribution of the magnetic field was measured by a Hall magnitometer. The uniformity of the magnetic field (up to 400 G) in a area of dusty structure was not worse than 5%. One of the modifications of the setup provided for shifting the tube along the coils. This allowed placing the dust structure into an area of both parallel and converging or diverging field lines.

The experiment was carried out in the following way. Dust particles were injected into the discharge. The magnetic field was gradually increased to avoid particles falling out from the discharge traps. Control observations were also performed in a decreasing and inverted magnetic field. In most cases Ne was the plasma-forming gas. In addition Ar, H_2, air, and mixtures of Ar and Ne with air and H_2 were used. Three types of particles were used: Al_2O_3 with a density of $\rho = 4.0\ \mathrm{g/cm^3}$, silicon with a density of $\rho = 2.5\ \mathrm{g/cm^3}$ and $LiNbO_3$ with a density $\rho = 4.6\ g/\mathrm{cm^3}$. All particle kinds were polydisperse. The size of $LiNbO_3$ granules was $1-4\ \mu$m.

The particles were illuminated by a 30 mW diode laser. We could visualize both structure as a whole and any of its sections with the help of a laser "knife." The "knife's" thickness was variable from 0.7 mm to 1 cm depending on the experimental demands. The scattered light was observed by a charge-coupled-device (CCD) video camera. The discharge glow was filtered out with an interference filter. The video camera could be placed above and on the side of the tube. Working pressure varied from 0.1 to 2 Torr; the discharge current varied from 0.5 to 6 mA.

In the magnetic field sufficient stability of plasma dust structures was attained at the approximate current 2 mA under 0.7 Torr pressure, the radii of tubes ranged from 1.1 to 1.6 cm. In order to increase the stability of discharge the cathode area was not effected by the longitudinal magnetic field of coils [29]. Moreover, the additional transversal magnetic field of several hundreds of gausses was applied by a permanent magnet between the cathode area and the diaphragm [30]. Under these conditions the discharge has distinct stratification, and running ionization waves are effectively suppressed. The standing strata are formed starting from the diaphragm toward the anode. The placement and number of strata in the observation area are changing with the application of a longitudinal magnetic field. We were able to make observations in the three closest to the diaphragm strata. In this paper we present the results of obser-

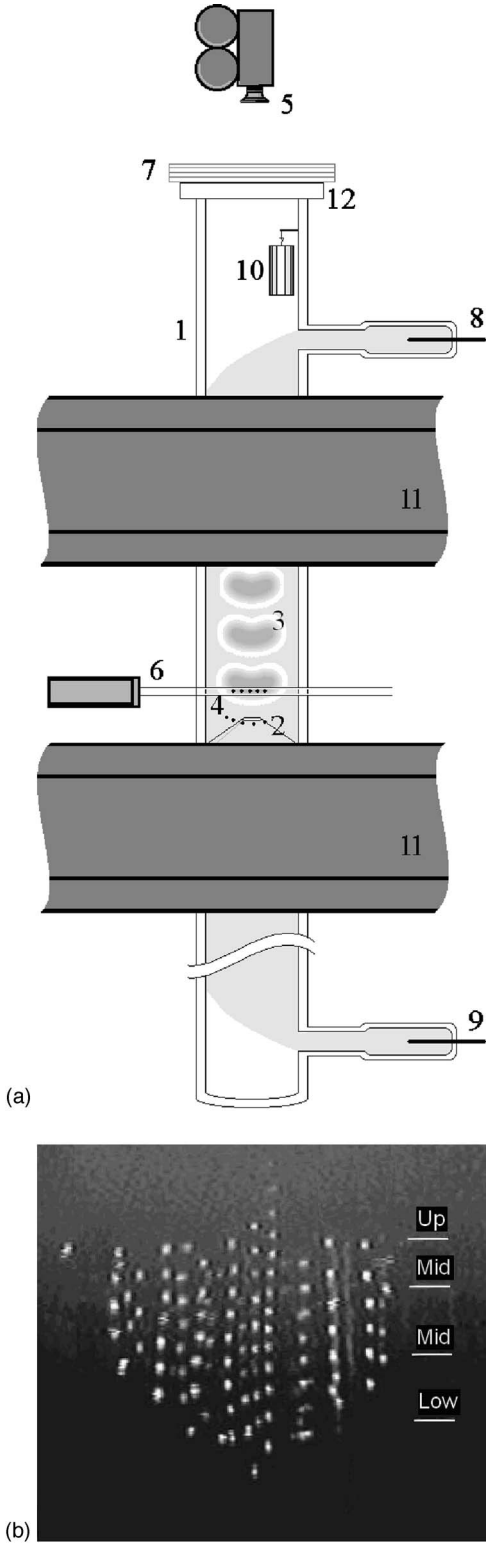

FIG. 1. (a) Experimental setup. 1: glass tube; 2: diaphragm; 3: strata; 4: levitated particles; 5: CCD camera; 6: system-forming laser knife; 7: filter; 8: anode; 9: cathode; 10: container with powder; 11: coils; 12: window. (b) A typical image of a vertical section of the structure. The vertical size of the image is 6.2 mm. The selected sections are indicated at the right. Gas discharge conditions: Ne under a pressure of 0.7 Torr; discharge current 2.5 mA; $LiNbO_3$ particles.

vations in the first stratum and in the one closest to the diaphragm area.

III. STUDYING OF ROTATIONAL MOTION

A. Observation of the dust structures rotation in strata

As mentioned above, rotational motion in a magnetic field in the glow discharge was revealed earlier [13,31]. The purpose of the present investigation is to study the effect of plasma flows on dust granules in a magnetic field. This effect can cause the gradient of the angular velocity of rotation. For such an observation the weakly ordered and stable dust structure is required. We succeeded to construct the required structure using particles of $LiNbO_3$. The pair-correlation function $g(r)$ for several horizontal sections of structure was calculated to control the ordering. A number of horizontal sections of the structure [Fig. 2(a)] with different vertical coordinates were selected. Figure 1(b) shows the vertical section of the dust structure at zero magnetic field. The arrangement order of dust particles can be different in various sections of the investigated three-dimensional structure. In this case it decreases from the upper to the lower layer (from the anode to the cathode, along with the current of the discharge) that shows Fig. 3(a). The structure prepared for research has the "long-range" ordering (the second and third peaks on $g(r)$, Fig. 3(a), are distinct) only in the upper layer.

In the presence of the magnetic field the dust structure starts to rotate. It rotates practically as a solid with an angular velocity up to 1 rad/s under the following conditions: Ne discharge, $i=2$ mA, $p=0.7$ Torr, B up to 100 G. The directions of the angular velocity $\boldsymbol{\omega}$ and the magnetic field $\mathbf{B}$ correlate as $\boldsymbol{\omega}\uparrow\downarrow\mathbf{B}$ to each other under these conditions. Since the projection of $\boldsymbol{\omega}$ on the direction of $\mathbf{B}$ is negative we shall attribute "negative" angular speed to such a rotation. Two phenomena were discovered with an increase of the magnetic field: nonmonotonic dependence $\omega(B)$ and the inversion of rotation direction. It is important that in the dc glow discharge inversion of the rotating direction occurs without external variations of discharge parameters: radial potential V_A in Refs. [10,20] or peak-to-peak rf voltage U_{pp} [12].

We denote the angular velocity for each horizontal section (not for the structure as a whole) as ω_{up}, ω_{mid}, and ω_{low}, and assume that $\omega(r)$ for each section is near a constant, Fig. 3(b). The angular velocity of a single particle is $\omega=v/r$. The angular velocity of a section $\langle\omega\rangle$ is calculated by averaging on the ensemble of particles and over the time of observation. Its error is related with the one of particle positioning and the determination of the rotation center. The functional dependence $\langle\omega\rangle$ (B) was calculated for three sections and shown in Fig. 4. The value B at which $\omega=0$ is denoted as B_0, separates "small" magnetic fields $B<B_0$ when $\boldsymbol{\omega}\uparrow\downarrow\mathbf{B}$ and "large" magnetic fields $B>B_0$ when $\boldsymbol{\omega}\uparrow\uparrow\mathbf{B}$.

The structure does not stop rotation as a whole at the value B_0 of magnetic induction. Different sections of the structure stop at different B_0. This effect becomes apparently distinct in the structures consisting of silicon polydisperse particles. The upper and lower sections simultaneously rotate

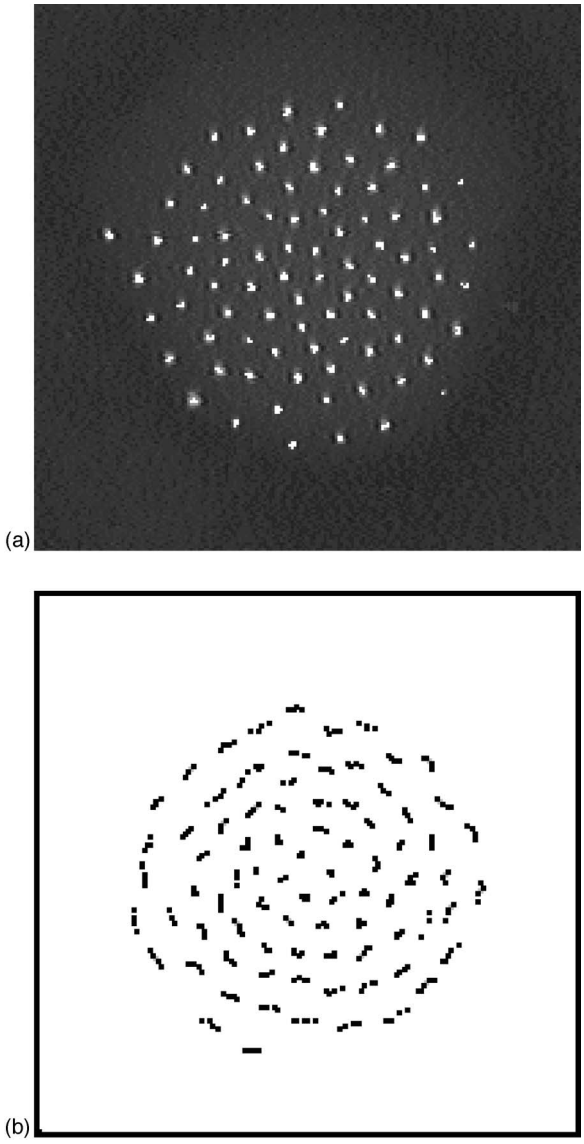

FIG. 2. (a) A typical image of a horizontal section [corresponding to "Up" in Fig. 1(b)] of the structure. The vertical size of the image is 4.2 mm. Gas discharge conditions: Ne under a pressure of 0.7 Torr; discharge current 2.5 mA; $LiNbO_3$ particles; magnetic field 28 G. (b) Rotation (clockwise) in the magnetic field. Four successive frames (five frames/s) are superimposed. The magnetic field is directed upward. The conditions and scale correspond to Fig. 2(a).

in the opposite directions ($\langle\omega\rangle_{up}<0$, $\langle\omega\rangle_{low}>0$) when $B\approx B_0$ and the vertical gradient of angular velocity is $\Delta\langle\omega\rangle/\Delta h=0.1$ rad/sec mm [32,33]. In small magnetic fields the gradient $\langle\omega\rangle$ is directed upwards ($\langle\omega\rangle_{up}>\langle\omega\rangle_{low}$), in large magnetic fields the gradient $\langle\omega\rangle$ is directed downwards ($\langle\omega\rangle_{up}<\langle\omega\rangle_{low}$). The rotation heterogeneity of structures consisting of $LiNbO_3$ particles is less evident and was registered by side view only.

The magnitude of the angular velocity reaches 3 rad/s ($v\approx 1$ cm/s) in the magnetic field of 350–400 G. As mentioned above, the value of a discharge current in experiences was about 2–2.5 mA. With the increase of the discharge

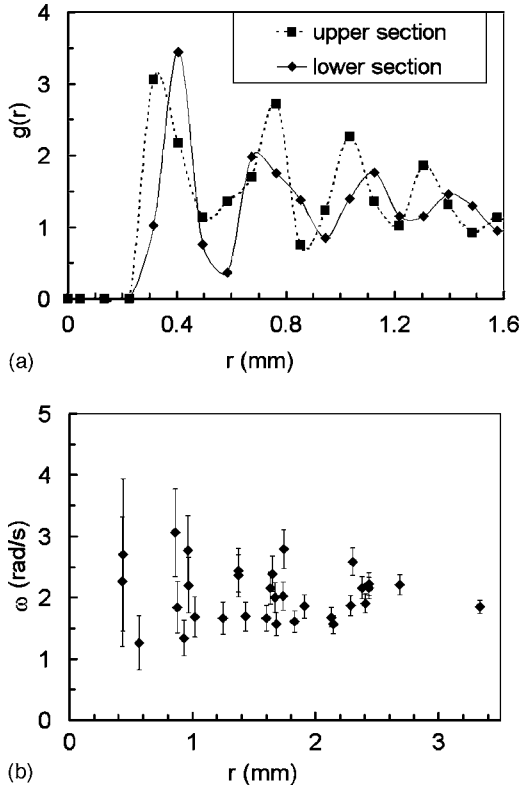

FIG. 3. (a) The pair-correlation function of the structure for the center areas of the upper and lower sections. Gas-discharge conditions: Ne under a pressure of 0.7 Torr; discharge current 2.5 mA; $LiNbO_3$ particles; the magnetic field is absent. (b) The dependence of the angular velocity of dust particles on the radial coordinate. Gas-discharge conditions: Ne under a pressure of 0.7 Torr; discharge current, 2.5 mA; $LiNbO_3$ particles; magnetic field 320 G. One of the lower sections of the structure.

current the angular velocity increases up to 8 rad/s, but the shape of the structure changes. In represented research the variation of a current was not carried out to avoid the dust-structure shape change.

B. Observation of rotation of dust structures nearby the diaphragm

Using the lightest particles (<1 microns, Al_2O_3, silicon) we can build the dust structure in the area above the diaphragm in the glow discharge. Such structures were observed earlier in Ref. [34]. These structures usually tend to form a ring in the magnetic field [13]. With the increase of the magnetic field the structure displaces aside to a wall of a tube, and then it decomposes and falls. In up to 100 G, the angular velocity is 3–5 rad/s (depending on a discharge current) and its direction is $\boldsymbol{\omega}\uparrow\uparrow\mathbf{B}$ (Fig. 5).

C. Shearing and melting

The inhomogeneous rotation of the 3D dust structure may cause its torsion deformation. In most cases particles line up in vertical lines (chains) in 3D structures [34–36] [Fig. 1(b)]. These chains are moving without destruction in high enough

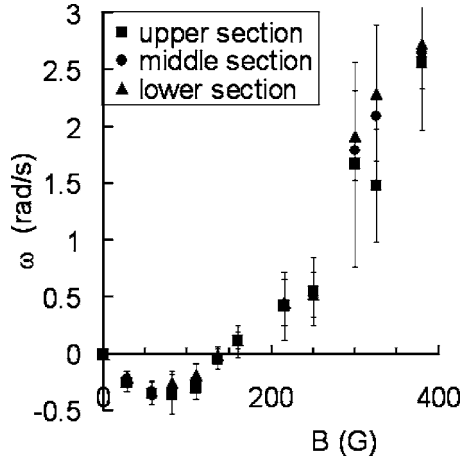

FIG. 4. Dependence of the average angular velocity of a dust structure on the induction of a magnetic field for different sections. Gas-discharge conditions: Ne under a pressure of 0.7 Torr; discharge current, 2.5 mA; $LiNbO_3$ particles. The inversion of the angular-velocity direction occurs at $B \approx 150$ G. Deviations from a smooth dependence correspond to somewhat of a deceleration of structure rotation due to the appearing (at 250 and 325 G) instability of discharge.

ordered rotating structures only. Their vertical alignment persists in the case of slow rotation. With the growth of ω their tilt occurs (torsion deformation of the structure). In Fig. 6 it is seen as shear in an illuminated vertical section.

The chains breakage begins with the appearance of an ω gradient. Figure 7 shows the vertical section of the rotating structure in $B \geqslant B_0$. Under these conditions the angular velocity is positive and its gradient is directed downwards. The outlined area in Fig. 7(a) shows melting caused by rotation heterogeneity. All chains here are broken. The dependence of velocity on the height coordinate h is shown in Fig. 7(b). It demonstrates that the upper part (h from 0 to 1.25 mm) moves like a solid and the lower part like a liquid.

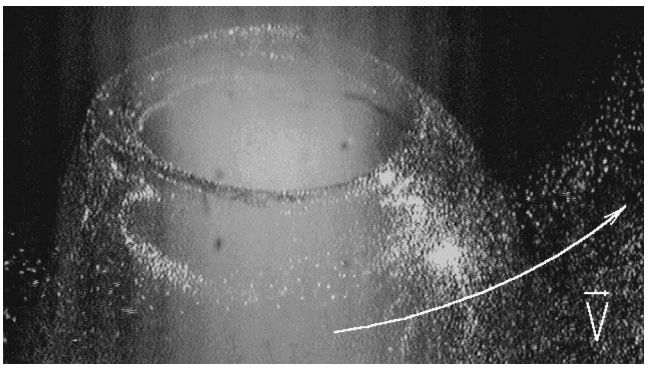

FIG. 5. Rotation of the ringlike dust cloud formed above the diaphragm in the magnetic field. The diaphragm and front part of the cloud are illuminated. Gas-discharge conditions: Ar under a pressure of 0.6 Torr; discharge current, 1.5 mA; Al_2O_3 particles; magnetic field 60 G. The inner radius of the ringlike cloud is 6.5 mm. The horizontal size of the image is 12 mm. The laser knife thickness is 1 mm. The video camera was arranged at an angle of 25° to the horizontal plane. The magnetic field is directed upward.

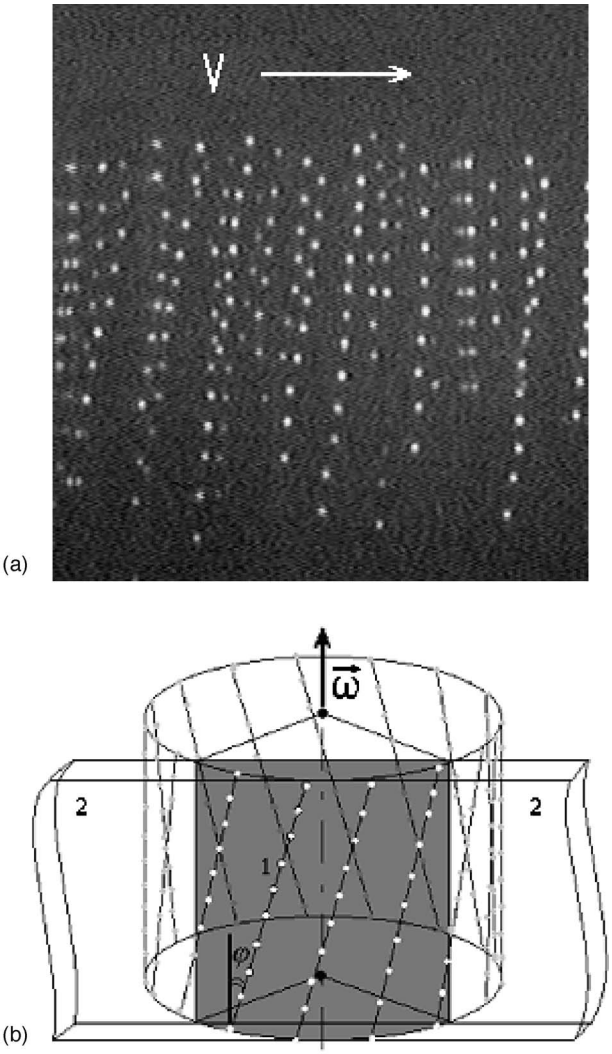

FIG. 6. (a) Vertical section of a rotating structure. The arrow specifies a direction of movement in $B<B_0$, $B=135$ G. The vertical size of the image is 2.8 mm. Illumination of one of the sections, located behind an axis of symmetry, a vertical plane thickness of 1 mm. Particles: $LiNbO_3$. Gas-discharge conditions: Ne (with a small impurity of air), $p=0.7$ Torr, $i=1.7$ mA. (b) Torsion deformation of the dust structure and the scheme of supervision. 1: shearing in a visualized plane 2.

D. Intermediate conclusions

As present results show, the behavior of dust structures in the magnetic field in glow discharge is rich with new physical effects contributing to the development of dusty-plasma physics. Further well try to investigate mechanisms of rotational motion and to estimate viscoelastic properties of dusty structures. The angular velocity is about a one to two order of magnitude larger than one in another discharge chamber [12,14,16] under comparable conditions.

The value of the magnetic induction B_0 increases with the growth of filling gas pressure and depends on its chemical composition. It slightly increases in small air admixture. At a magnetic-field induction of 135–150 G, at which the structure stops rotating, only electrons are magnetized: $\Omega_e \tau_e \approx 1$, where Ω_e is the cyclotron frequency and τ_e is the time between electron collisions.

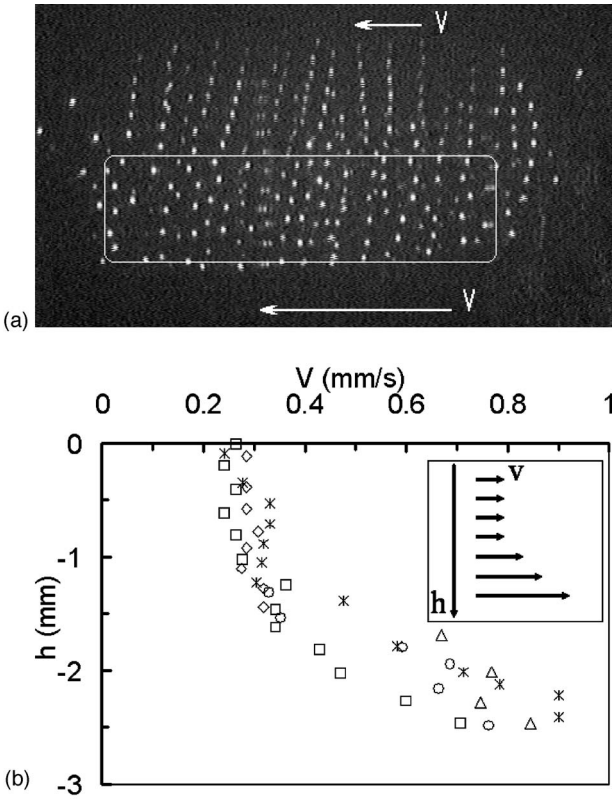

FIG. 7. (a) The image of a vertical section of a rotating structure. The arrow specifies a direction of rotation ($B=300$ G). The size of the image on a vertical is 2.8 mm. Illumination of one of the sections, located behind an axis of symmetry, a vertical plane thickness of 1 mm. Particles: $LiNbO_3$. Conditions: Ne (with a small impurity of air), $p=0.7$ Torr, $i=1.7$ mA. The magnetic field is directed upwards. An outlined area shows melting caused by rotation heterogeneity; all chains here are broken. (b) The dependence of velocity on height coordinate h. The insert shows the vertical gradient of velocity. Different data markers correspond to different chains of particles.

The investigation of the possible reasons of rotational motion was carried out in Refs. [25,38]. We suppose that the reason for the rotational motion is doubtless the ion-drag force [18,37]. A similar explanation of the dust structures rotation mechanism in other discharge types was made in Refs. [12,17].

In the small magnetic field $B<B_0$ the rotation of the dust structure relates with the radial ion flow directed from tube axis. In the large magnetic field $B>B_0$ the rotation of the dust structure relates with the radial ion flow directed from the wall to the axis of the discharge tube. For the structures situated above the diaphragm this radial flow is caused by the narrowing of the discharge current channel. In order to clarify the question about the possible existence of plasma flows in strata directed from the tube wall to an axis, two additional experiments were carried out.

IV. INTERPRETATION OF ROTATIONAL MOTION

A. Onset of rotational motion (additional experiment)

In order to initiate the rotation of an originally standing structure one can increase magnetic induction and/or dis-

charge current. The increase of B and i is accompanied by a change of structure shape and vertical position. It is an obstacle to the continuous observation of rotation onset. We have found another way of "turning on" and "turning off" the rotation in conditions of a certain value of B. It is comprised of the displacement of the dust structure from the discharge tube axis. As it was discovered in Refs. [25,35], a rather small displacement of the structure due to discharge tube tilting for about 10° with respect to the vertical stops rotation. We displaced the rotating structure by applying a double influence of the magnetic field summed with either a gravity component or thermophoresis force [39]. Omitting the experiment details (see Ref. [38]), below we present the obtained results for the cases of small and large magnetic fields separately.

1. Observation in small magnetic fields

In the experiment, the upper section of the structure was illuminated and videotaping was done from above. The upper section was chosen because, in small magnetic fields, it rotates with a greater angular velocity ($\langle\omega\rangle_{up} > \langle\omega\rangle_{low}$). The discharge conditions were maintained such that the angular velocity of the rotation of the top of the structure was about 0.5 rad/s. Then, the structure was displaced from the axis of the discharge tube at such a distance (a few millimeters) that the rotation ceased, and the structure spontaneously returned to the symmetry axis of the tube. We observed that, when the structure was displaced by some distance from the axis of the discharge tube, vortices began to form in *the structure center* [Fig. 8(a)]. Each vortex consisted of several particles rotating around a vertical axis. One or several vortices could form. Over the course of time, vortices could move, vanish, and arise in other places or combine with other vortices. The particles were set in rotation in vortices within a few seconds. As the dusty structure approached the center of the discharge, the vortices combined to form a solitary vortex. Then, this solitary vortex entrained all the remaining particles.

2. Observation in large magnetic fields

In the experiment, the lower section of the structure was illuminated, because it rotates with a greater angular velocity, in large magnetic fields ($\langle\omega\rangle_{up} < \langle\omega\rangle_{low}$). Our observations show that the onset of dusty-structure rotation begins from its *peripheral region*. Figure 8(b) shows stationary rotation by means of several superimposed frames; the particles in the central region are at rest.

Thus in small magnetic fields the rotation begins in the central part of the structure's upper section, whereas in large magnetic fields it begins on the periphery of the lower section.

B. Numerical estimations

1. Ion-drag-force estimation

Let us estimate the characteristic value of the velocity of an ion flow that causes the rotation of a dust structure with a constant angular velocity of 1 rad/s. Consider a single-layer

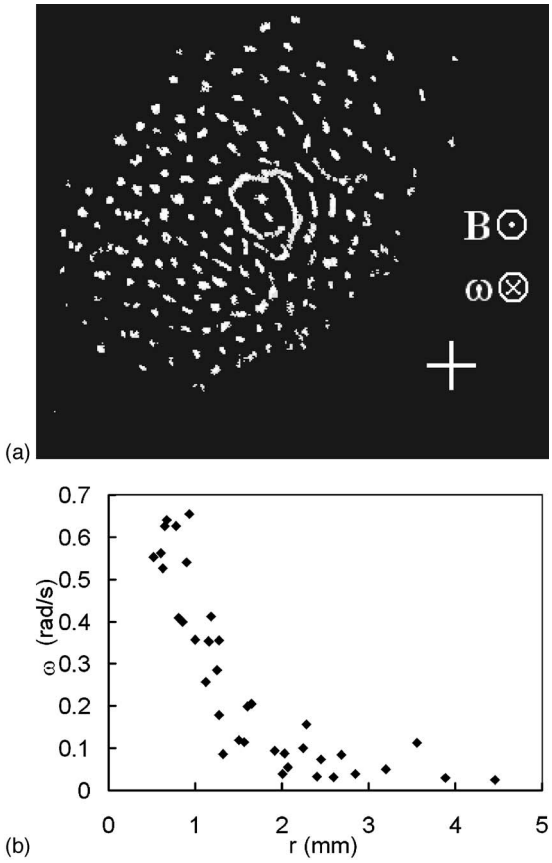

FIG. 8. Onset of the rotational motion of the dust structure displaced from the discharge axis, top view (first additional experiment). Particles: $LiNbO_3$. Conditions: Ne, $p=0.7$ Torr, $i=2.5$ mA. (a) $B=110$ G. The size of the image on a vertical is 8.3 mm. The tube axis is designated by a cross. (b) The dependence of the particle angular velocity on the distance from the center of the vortex [corresponding to Fig. 8(a)]. (c) $B=380$ G. The size of the image on a vertical is 3.5 mm.

structure uniformly rotating around its symmetry axis with an angular velocity ω. In the steady-state case, the torque of friction forces should equalize the torque that rotates the structure. Among external azimuth forces acting on the structure, only the ion-drag force F_{id}^{φ} and the force of neutral gas friction F_N^{φ} [40] are present. We will not consider the forces of interparticle interactions because they are internal forces and do not change the angular momentum of the structure. Then,

$$\sum rF_N^{\varphi} = \sum rF_{id}^{\varphi}, \tag{1}$$

where the summation should be performed over all the particles of the structure. The moment of the force F_{id}^{φ} can be easily calculated. In contrast, the exact calculation of the moment of the force F_N^{φ} is difficult since the radial distribution of the parameters that determine the drag force in the region of location of the dusty plasma structure is unknown [12,18].

For the simplified estimation, we will consider a single dusty particle that moves independently of the other particles of the structure. Upon uniform azimuth motion of this par-

ticle, the friction force equalizes the drag force. Let the particle be located at the average radius of the structure r_{av}. Then, for this particle,

$$F_N^{\varphi} = F_{id}^{\varphi}. \tag{2}$$

The friction force is proportional to the velocity of the particle and relative to the surrounding gas: $F_N = k_n u_d$ (here, k_n is a constant that is determined by the gas pressure, the size and shape of the particle, and the interaction of atoms with the particle surface). Since the used particles were arbitrary in shape, the coefficient k_n was determined experimentally. We observed the trajectories of falling particles at a distance of 30 cm from the container (with the discharge switched off). At this distance, the vertical motion of the particles was steady state. Then $k_n = m_d g / u_d$ (m_d is the mass of a dusty particle). The region of observation was illuminated from above through an end window, while videotaping was performed through the sidewall of the discharge tube. The coefficient k_n was determined for $LiNbO_3$ particles in Ne under a pressure of 0.7 Torr. The measured velocities of particles were in the range 2–8 cm/s. The scatter in the velocity was caused by the scatter in the size of particles. For the lightest particles, we found that $k_n = 10^{-12}$ kg/s. Our observations of the formation of dusty-plasma structures give grounds to assume that the structures are mainly formed by the lightest particles. If u_d is the linear velocity of a particle that is located at the average radius of a rotating structure, then $u_d = \omega r_{av}$. We will consider dust structures having a diameter of 0.4 cm and rotating with an angular velocity of 1 rad/s, which corresponds to the conditions of most experiments. In this case, the friction force is $F_N \approx 10^{-15} N$.

We will estimate the ion-drag force two ways. First, we will use the simplest model of Ref. [18]. The expression for the ion-drag force can be represented in the form $F_{id}^{\varphi} = k_i v_{i\varphi}$, where $v_{i\varphi}$ is the azimuth component of the velocity of the ion flow. The coefficient k_i depends on the ion concentration n_i, the charge of the dusty particle Ze, and the value $v_{\Sigma} = \sqrt{\frac{8kT_i}{\pi m_i} + {v_{i\varphi}}^2}$ (m_i and T_i are the ion mass and ion temperature, respectively). Assuming that $n_i = 10^{15}$ m^{-3}, $m_i = 2 \times 10^{-26}$ kg and $v_{\Sigma} \approx 10^3$ m/s, we find that, depending on the ratio between the velocities of the ordered and thermal motions of ions, the value of the coefficient k_i lies in the range $10^{-15} - 10^{-14}$ kg/s.

Apart from the theoretical estimation of the proportionality coefficient k_i, we estimated this coefficient based on the experimental data from Ref. [41], where, under conditions similar to ours, the ion drag force was measured in the positive column of a dc glow discharge in Ne. Knowing the longitudinal electric field (i.e., the velocity of the ion flow) and the measured ion-drag force acting on probe particles, one can calculate the proportionality coefficient between them. Such an estimation yields a value of the same order for the coefficient k_i as the theoretical estimation does.

Substituting the forces F_{id}^{φ} and F_N^{φ} into Eq. (2), we find that the rotation of a dust structure with an angular velocity $\omega = 1$ rad/s can be caused by an ion flow whose azimuth velocity component is $v_{i\varphi} = 0.1 - 1$ m/s. The radial and azimuth components of the velocity of an ion flow, v_{ir} and $v_{i\varphi}$, are related by the expression [27,29]

$$v_{ir} = \frac{v_{i\varphi}}{\Omega_i \tau_i}, \tag{3}$$

where τ_i is the time between collisions of ions with gas atoms and Ω_i is the cyclotron frequency of ions. Under our conditions, $\Omega_i \tau_i \approx 0.01$; then we obtain the following estimate for the radial velocity: $v_{ir} = 10 - 100$ m/s.

As will be shown below, a radial ion flow with such a velocity can be caused, e.g., by a radial electric field E_r. The radial field strength $E_r = 0.3 - 3$ V/cm obtained in this way is plausible for the central discharge region.

2. Elastic shear modulus

The above fulfilled estimations of ion-drag force provide for the calculation of the elastic-shear modulus of the dust crystal shown in Fig. 6. Let's make these estimations according to a standard mechanical model. According to Fig. 6 an average angle of an inclination of chains $\varphi = 10°$, relative shift $\gamma = 0.2$. The elastic-shear modulus is connected with a stress τ: $\tau = G_{sh}\gamma$. The reason for τ appearance is the ion-drag force F_{id}. The area S ($\tau = F_{id}/S$) is supposedly equal to 0.2×10^{-4} m^2. The estimated characteristic value for the elastic modulus G_{sh} is 10^{-6} dyn/cm^2.

3. About the plasma flows towards the dust structure in the magnetic field

Our observations of the displacement of a structure from the symmetry axis in small magnetic fields allow us to make the following conclusions. If the rotation of a structure is associated with radial ion flows toward the tube wall, then it is likely that these flows arise in the dust structure itself. Indeed, under certain conditions, the dusty-plasma structure can generate a flow from its internal regions to the periphery. The dusty particles forming the structure have a large negative charge (in our case, its value was estimated to be as large as 10^4 elementary charges). If the concentration of dusty particles is sufficiently high, the charge of electrons located in the region of existence of the structure will be neutralized at the particle surface (rather than as a result of diffusion to the tube wall). For the quasineutrality of the plasma within the dusty structure to be retained, the frequency of ionization should increase. The possibility of this was discussed in Refs. [3,34]. In this case, due to the concentration gradient formed, the radial ion flow is directed from internal regions of the structure to its periphery. One can estimate the radial velocity v_{ir} that ions acquire as a result of diffusion. From the quasineutrality condition for a dusty plasma [4], it follows that

$$n_i = n_e + Z n_d. \tag{4}$$

Here, n_d is the concentration of particles in the dusty structure. According to our measurements, $n_d = 3.7 \times 10^{10}$ m^{-3}. The charge of a dusty particle and the concentration of electrons were estimated according to Refs. [34,42]: $Z \approx 10^4$, $n_e = 10^{14}$ m^{-3}. The concentration of ions in the cloud $n_i = 5 \times 10^{14}$ m^{-3}. The velocity of the ion flow arising from

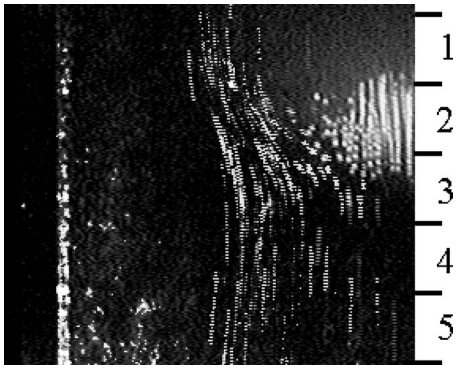

FIG. 9. Gravity-driven probing of strata (second additional experiment). Trajectories indicating the area of probing (side view). At the right the illuminated horizontal layers (1–5) are shown. The size of the image on a horizontal is 15 mm. Gas discharge conditions: Ne under a pressure of 0.7 Torr; $B=0$; laser knife thickness is 1 mm.

$$v_{ir} = \frac{D_i}{n_i}\frac{dn_i}{dr}, \tag{5}$$

where the coefficient of the diffusion of ions $D_i=0.01$ m^2/s [26]. For the dusty structure with a radius of 5 mm, the $v_{ir} \approx 10$ m/s. This is consistent with the estimates made above.

If the displacement of a structure from the tube axis is considerable, the structure stops rotating. If the structure were subjected to flows caused by an ambipolar field, it probably would keep on rotating around the symmetry axis of the tube. The appearance of vortices in the internal region of a structure and their direction, as well as the continuous motion of the center of rotation, can indicate that, *due to the diffusion, outward flows arise in the internal region*.

Our observations of the onset of the rotation of a structure *in large magnetic fields* allow us to state the following. The rotation of a structure begins from its periphery. This means that, evidently, a component of the ion flow directed *toward the structure* exists in a large magnetic field. The relation of this flow with a *radial electric field* was investigated in the following experiment.

C. Gravity-driven probing of strata (additional experiment)

It is necessary to find out the reason for the radial plasma flow towards the tube axis in $B \geqslant B_0$ and to define the spatial area of this flow. If the reason for the flow is the locally inversed electric field the gravity-driven probe grains will detect it [43]. The experiment checking of this assumption was carried out in the experimental setup mentioned above. We investigated the horizontal and vertical trajectory projections in conditions: $B=0$; $B<B_0$; $B>B_0$; with the structure in stratum and without it [44]. In order to define the direction and magnitude of the radial electric field in stratum it is enough to interpret the azimuth projection of probe particle trajectories.

First of all let us show the character of particle trajectories without the magnetic field. The trajectories shown in Fig. 9 indicate the area of probing. Two areas of probe particles are falling uniformly. In the first area particles accelerate towards the tube axis and upwards, simultaneously. In the second area particles accelerate towards the tube wall and downward simultaneously [45]. In the discharge with $i=2$ mA, $p=0.7$ Torr, Ne, $LiNbO_3$, average measured accelerations without the magnetic field $w_r=12$ cm/s^2, $w_h=25$ cm/s^2. Their magnitudes slightly decrease in the magnetic field applied. Thus a three-dimensional character of motion should be taken into account in observation of azimuth trajectories projections in the magnetic field.

1. Observations in small magnetic fields

The magnetic field was directed upwards and varied from 0 up to 150 G. The visualization area was divided into five layers (Fig. 9). Observations were consequently performed in each of them. Figure 9 schematically shows the falling particles stream. Qualitative observations are as follows. In layers 1–3 probe particles are deviated clockwise in all diapasons of small magnetic fields. In layers 4 and 5 particles have no any azimuth deviations in magnetic fields up to 100 G. With the growth of B higher than 100 G azimuth counterclockwise deviations are induced first in layer 5 and then in layer 4. Figure 10(a) schematically shows the horizontal trajectory projection of a probe particle in the *presence of the dust structure in stratum*. Quantitative results for $B=120$ G are tabulated (Table I).

Observations of falling particles in the same conditions *with no structure formed in stratum* were also carried out. The qualitative results are as follows. In layer 1 probe particles deviate clockwise in all diapasons of small magnetic fields. In layers 2 and 3 azimuth deviations are absent. This is a *principal difference* from the case when the structure is present in stratum. In layers 4 and 5 the azimuth deviation of probe particles is counterclockwise and the velocity of this motion increases with the magnetic field. Figure 10(b) schematically shows horizontal trajectory projection of the probe particle in the absence of the dust structure in a stratum. Quantitative results for $B=120$ G are tabulated (Table I).

2. Observations in large magnetic fields

Observations were carried out in the same layers with magnetic fields of 300–400 G in the presence and absence of a structure in the stratum (see Fig. 9). However, the dust-structure influence on the probe particles was not registered. The qualitative results are as follows. In layer 1 probe particles deviate clockwise. In layer 2 the deviations are either counterclockwise or not registered. This depends on the particles mass and distance from the tube axis. In layers 3–5 the deviations are counterclockwise and its velocity is higher in the lower layers. Figure 10(c) schematically shows the horizontal trajectory projection of the probe particle. The quantitative results for $B=350$ G are tabulated (Table I).

The formulas [Eqs. (2) and (3)] allow binding the values of the radial electric field E_r and azimuth velocity of probing particles. Let us estimate the value of E_r using the expression $v_{ir}=b_iE_r$, where $b_i=0.3$ m^2/(s V)—ion mobility under the given conditions [26], as

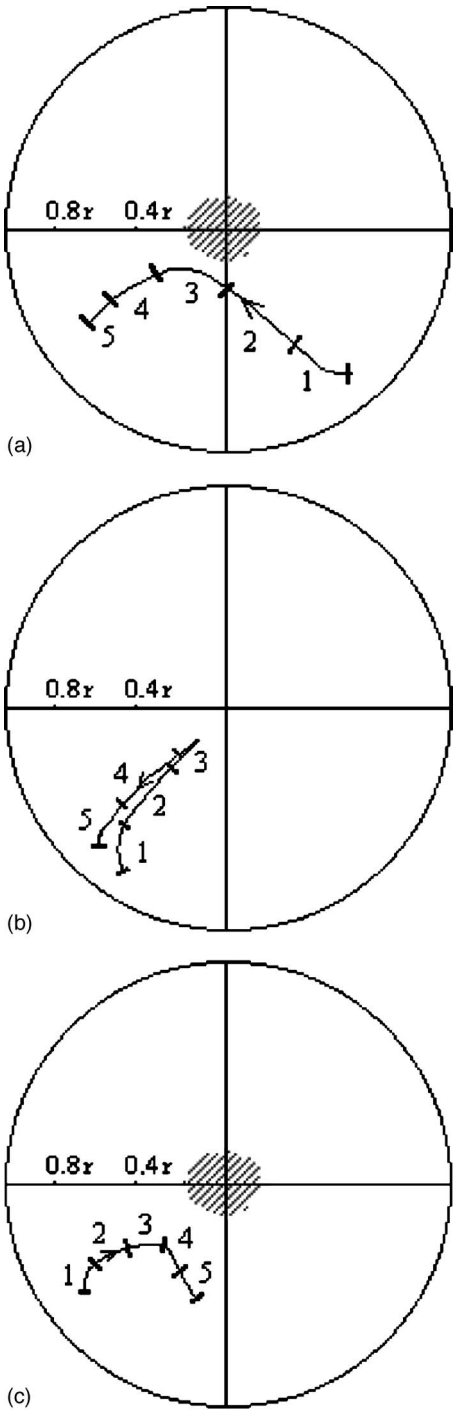

FIG. 10. Sketch of the horizontal trajectory projection of the probe particle (top view). (a) $B<B_0$, the case of the presence of the dust structure in stratum (shading shows the dust structure). (b) $B<B_0$, the case of the absence of the dust structure in stratum. (c) $B>B_0$ (shading shows the dust structure). Curves are divided into segments (1–5) corresponding to different layers (Fig. 9).

$$E_r = \frac{k_n v_d^{\varphi}}{k_i b_i \Omega_i \tau_i}. \tag{6}$$

Estimations of E_r by Eq. (6) are as follows. In the case of a small magnetic field (120 G) in layer 1, E_r=3.3 V/cm (at r=9 mm); in layer 5, E_r=−0.8 V/sm (at r=7 mm). The minus corresponds to the inversion of a field in this area of the discharge. In the case of the large magnetic field (350 G) in layer 1, E_r=0.9 V/cm (at r=10 mm); in layer 5, E_r=−0.6 V/cm (at r=10 mm).

TABLE I. Results of gravity-driven probing. The layers correspond to Fig. 9. The presence (absence) of a dust structure is designated by + (−). Probing particles are influenced by the dust structure in layer 2 at 120 G.

B	Section	r (mm)	ω (rad/s)	Structure	Direction
$B<B_0$	1	9	1.1	+,−	$\boldsymbol{\omega}\uparrow\downarrow\mathbf{B}$
(120 G)	2	7.5–9.5	0.6	+	$\boldsymbol{\omega}\uparrow\downarrow\mathbf{B}$
		6.5–8.5	0	−	
	3	6.5–9.5	0	+,−	
	4	6.5–9.5	0	+	
			0	−	
	5	6–8	0.4	+,−	$\boldsymbol{\omega}\uparrow\uparrow\mathbf{B}$
$B>B_0$	1	10	0.8	+,−	$\boldsymbol{\omega}\uparrow\downarrow\mathbf{B}$
(350 G)	2, 3	10	0	+,−	
	4	8	0.5	+,−	$\boldsymbol{\omega}\uparrow\uparrow\mathbf{B}$
	5	10	0.6	+,−	$\boldsymbol{\omega}\uparrow\uparrow\mathbf{B}$

It should be mentioned that the inversion of E_r does not occur near the tube wall (and of course in the area containing the dust) structure in magnetic fields up to 400 G. This was confirmed by additional observations of the probing particles deviated towards the tube wall by the thermophoresis force (induced by walls cooling). Probably, the areas of inversed radial field exist in the stratum without the magnetic field applied too. The increase of the magnetic field causes the mentioned area to "lift" from layer 5 to layer 3. The existence of such areas in the absence of the magnetic field is discovered in Ref. [46]. Under similar conditions but in running strata at a certain phase the radial potential minimum is localized at r from 4 to 8 mm (not at the discharge axis).

V. CHANGES OF THE INTERIOR STATE OF THE DUST STRUCTURE

As follows from the investigations mentioned above the behavior of the dust structures in the glow discharge with the magnetic field applied is accompanied by the rich spectrum of physical phenomena, which can be closely related with intensive plasma flows at the dust granules. And by means of the external magnetic-field manipulation one can control plasma flows changing the internal structure of the plasma dust formation.

The influence of the magnetic field on the spatial arrangement of dusty particles can be qualitatively estimated by a comparison of the behavior of pair-correlation functions of the same structure in the magnetic field and in its absence. Figure 11 shows the dynamics of its change in the upper (a) and lower (b) sections with B=0, 28, and 160 G. Comparing the behavior of $g(r)$ (shown in these figures) one can see the destruction of "long-range" ordering in the upper section and

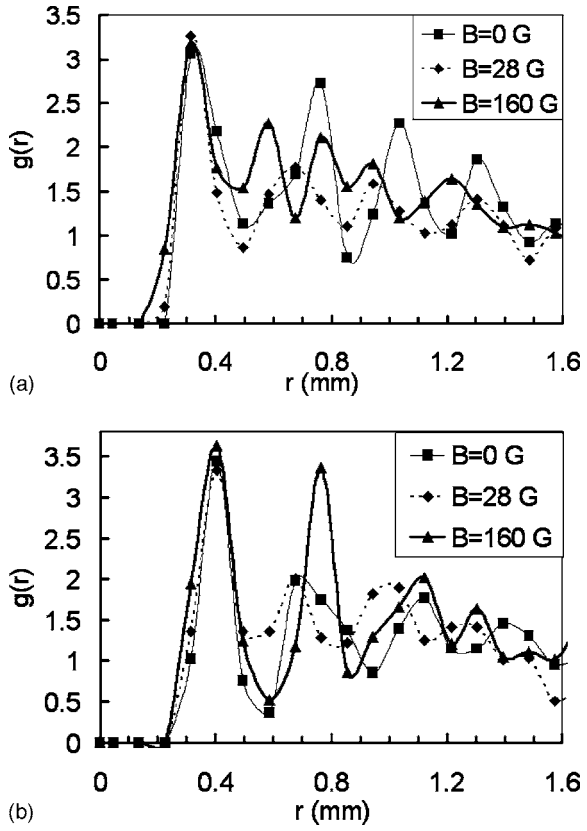

FIG. 11. Changes of the pair-correlation function for horizontal sections with a variation of the magnetic field. In the upper section (a) the second and third peaks are distinct only at $B=0$. In the lower section (b) the second peak appears at $B=160$ G. The interparticle distance remains constant in each horizontal section in magnetic inductions up to 400 G.

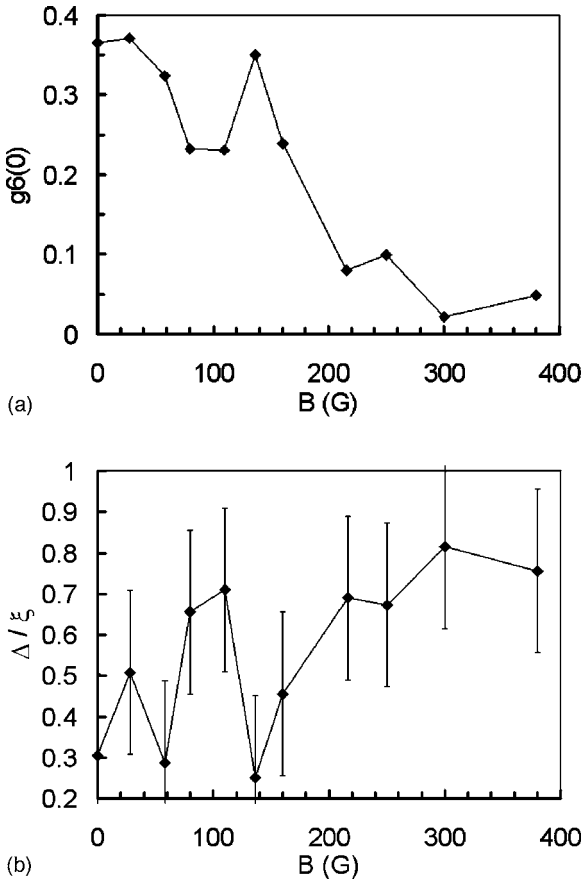

FIG. 12. Dependence of local orientational parameter $g_6(0)$—(a) and transitional parameter Δ/ξ—(b) on the induction of the magnetic field. In the diapasone of 0–400 G both parameters indicate the ordering decrease. The ordering increase occurs at 140 G ($B \approx B_0$, $\langle\omega\rangle \approx 0$).

the ordering increase in the lower section with induction B nearby B_0, and at $B=300$ G a complete destruction of long-range ordering may be easily identified. The special tools developed for the dusty plasma was applied for a quantitative investigation of the structure sections.

First, the pair-correlation function [47] $g(r)$ (with its three-parametric approximation [48]) and bond-orientational correlation function $g_6(r)$ [47] were calculated. These showed [49] that in our conditions according to the Kosterlitz-Thouless-Halperin-Nelson-Young (KTHNY) theory [50] the state of the dust structure is changing from almost hexatic to a gaseous disordered state with an increase of magnetic induction. It is possible that this approach is not the most informative under these conditions, but still it allows us to reveal the fact of structure melting.

Second, the local correlation functions [51–53]—the transitional order parameter Δ/ξ and orientational order parameter $g_6(0)$—were determined for all sections and magnetic-field values. The calculated values of $g_6(0)$ are shown in Fig. 12(a). For B values less than 160 G it weakly varies in value from 0.25 to 0.4. In magnetic fields higher than 200 G it falls to 0.05. The translational parameter is also changing [see Fig. 12(b)], but the character of its change in contrast to one of $g_6(r)$ is rather gradual. The following interpretation may be suggested. The structure has a disordered state in large magnetic fields and it is close to the liquid-ice and oscillating-phases boundary in small magnetic fields. Thus following the approach of Refs. [51,52] we suppose that the magnetic field induces melting of the dust structure in glow discharge.

Third, we tried to detect the polymorphic transformation with an increase of the magnetic field. This work concerns dust structures with short dimensions (10–12 lattice periods in diameter), low order, and high heterogeneity. That is why we can only arbitrarily assign them any crystal-lattice type. The comparison of $g(r)$ of the structure sections with pair-correlation functions of ideal 2D lattices shows the presence of both "hexagonal" and "cubic" lattices elements [45]. Besides, we compared the areas of structure sections occupied by cells of shape close to squares and hexagons [49]. Both methods show the decrease of the cubic phase part with the increase of B up to B_0. In a further increase of B the phase identification by this third approach does not seem possible.

VI. CONCLUSION

Our detailed investigation of the action of a magnetic field within the induction range 0–400 G on a dust structure in

strata allowed us to reveal several new results.

The dependence of the angular velocity on the magnetic field is nonmonotonic. The rotation direction inverses: at small magnetic fields $B < B_0$, $\boldsymbol{\omega} \uparrow \downarrow \mathbf{B}$; whereas, at large magnetic fields $B > B_0$ and $\boldsymbol{\omega} \uparrow \uparrow \mathbf{B}$. In experiment conditions B_0 is about 150 G. The angular velocity is about one to two orders of magnitude larger than one in another discharge chamber under comparable conditions.

The detection of an angular velocity gradient and its change in the magnetic field as well as the additional experiments on observations of rotation onset and on gravity-driven probing provided us with an investigation of the rotational motion mechanism. The reason for rotation motion is the action of the ion-drag force which is supported by simple estimations.

In the small magnetic field $B < B_0$ the rotation of the dust structure relates with the radial ion flow directed from the center of the structure. The presence of the dust structure effects the formation of flow. In the large magnetic field $B > B_0$ the rotation of the dust structure relates with the radial ion flow directed from the wall to an axis of the tube. It may be the result of local inversion of the radial electric field in the stratum. Our experiments showed no influence of the structure on the flow formation in $B > B_0$.

The magnetic field changes an order of the horizontal sections of the dust structure and causes the structure's melting. The observations of shearing allowed us to estimate the elastic shear modulus of the plasma dust crystal.

ACKNOWLEDGMENTS

We thank Aleksey V. Ivanov for helpful discussion. V.Yu.K. acknowledges financial support from the Ministry of Education and Science of the Russian Federation and the U.S. Civilian Research & Development Foundation (Grant No. RUX0-000013-PZ-06).

[1] P. K. Shukla and A. A. Mamun, *Introduction to Dusty Plasma Physics* (IOP, Philadelphia, 2002).
[2] *Dusty Plasmas: Physics, Chemistry, and Technological Impact in Plasma Processing*, edited by A. Bouchoule (Wiley, New York, 1999).
[3] V. E. Fortov, O. F. Petrov, and V. I. Molotkov *et al.*, Usp. Fiz. Nauk **174**, 427 (2004).
[4] V. N. Tsytovich, G. E. Morfill, and H. Thomas, Plasma Phys. Rep. **28**, 623 (2002).
[5] G. E. Morfill, V. N. Tsytovich, and H. Thomas, Plasma Phys. Rep. **29**, 1 (2003).
[6] H. Thomas, G. E. Morfill, and V. N. Tsytovich, Plasma Phys. Rep. **29**, 895 (2003).
[7] J. H. Chu and I. Lin, Phys. Rev. Lett. **72**, 4009 (1994).
[8] N. V. Tsytovich, N. Sato, and G. E. Morfill, New J. Phys. **5**, 43 (2003).
[9] K. Fukagawa, G. Uchida, S. Iizuka, and N. Sato, XXV IC PIG. 3, 37 (Nagoya, Japan, 2001).
[10] N. Sato, in *Dusty Plasmas in the New Millenium*, edited by R. Bharuthram *et al.*, AIP Conf. Proc. No. 66 (AIP, New York, 2002).
[11] N. Sato, G. Uchida, T. Kaneko, S. Shimizu, and S. Iizuka, Phys. Plasmas **8**, 1786 (2001).
[12] U. Konopka, D. Samsonov, A. V. Ivlev, J. Goree, V. Steinberg, and G. E. Morfill, Phys. Rev. E **61**, 1890 (2000).
[13] E. S. Dzlieva, V. Yu. Karasev, and A. I. Eikhval'd, Opt. Spectrosc. **92**, 943 (2002).
[14] F. Cheung, Al. Samarian, and B. James, New J. Phys. **5**, 75 (2003).
[15] E. S. Dzlieva, V. Yu. Karasev, and A. I. Eikhval'd, Opt. Spectrosc. **98**, 569 (2005).
[16] G. Uchida, R. Ozaki, S. Iizuka, and N. Sato, in Proceedings of the 15th Symposium on Plasma Processing (Japan, Hamamatsu, 1998), p. 152.
[17] P. Kaw, K. Nishikawa, and N. Sato, Phys. Plasmas **9**, 387 (2002).
[18] M. S. Barnes *et al.*, Phys. Rev. Lett. **68**, 313 (1992).
[19] S. Nunomura, N. Ohno, and S. Takamura, Jpn. J. Appl. Phys., Part 1 **36**, 877 (1997).
[20] K. Fukagawa, G. Uchida, S. Iizuka, and N. Sato, XXV IC PIG. 3, 39 (Nagoya, Japan, 2001).
[21] S. V. Vladimirov and M. Nambu, Phys. Rev. E **52**, R2172 (1995).
[22] S. V. Vladimirov and O. Ishihara, Phys. Plasmas **3**, 444 (1996).
[23] S. V. Vladimirov, S. A. Maiorov, and N. F. Cramer, Phys. Rev. E **63**, 045401(R) (2001).
[24] S. V. Vladimirov, K. Ostrikov, and A. A. Samarian, *Physics and Applications of Complex Plasmas* (Imperial College, London, 2005).
[25] E. S. Dzlieva, V. Yu. Karasev, and A. I. Eikhval'd, Opt. Spectrosc. **97**, 107 (2004).
[26] Yu. P. Raizer, *Gas Discharge Physics* (Springer, Berlin, 1991).
[27] V. E. Golant, A. P. Zhilinskii, and S. A. Sakharov, *Fundamentals of Plasma Physics* (Wiley, New York, 1980).
[28] P. S. Landa, N. A. Miskinova, and Y. V. Ponomarev, Usp. Fiz. Nauk **132**, 61 (1980).
[29] V. L. Granovskiy, Current in Gas (Nauka, Moskva, 1971), in Russian.
[30] B. N. Klarfeld, Zh. Eksp. Teor. Fiz. **22**, 66 (1952).
[31] E. S. Dzlieva, V. Yu. Karasev, and A. I. Eikhval'd, in *Proceedings of the Conference on Physics of Low Temperature Plasma, Part 2*, (Petrozavodsk, 2001), p. 115 (in Russian).
[32] E. S. Dzlieva, V. Yu. Karasev, and A. I. Eikhval'd, in *Proceedings of the Conference on Physics of Low Temperature Plasma, Part 1* (Petrozavodsk, 2004), p. 265 (in Russian).
[33] E. S. Dzlieva, V. Yu. Karasev, and A. I. Eikhval'd, in *Laser Research in St. Petersburg State University* (St. Petersburg Gos. University, St. Petersburg, 2003), p. 286.
[34] A. M. Lipaev *et al.*, JETP **85**, 1110 (1997).
[35] A. I. Eichvald, V. Yu. Karasev, and E. S. Dzlieva, in *Proceedings of the 4th International Conference on Plasma Physics & Plasma Technology* (Minsk, 2003), p. 256.
[36] A. I. Eichvald, V. Yu. Karasev, and E. S. Dzlieva, in *Proceed-*

ings of the 5th International Conference on Plasma Physics & Plasma Technology (Minsk, 2006), p. 428.
[37] S. A. Khrapak, A. V. Ivlev, G. E. Morfill, and H. M. Thomas, Phys. Rev. E **66**, 046414 (2002).
[38] E. S. Dzlieva, V. Yu. Karasev, and A. I. Eikhval'd, Opt. Spectrosc. **100**, 456 (2006).
[39] V. V. Balabanov, L. M. Vasilyak, and S. P. Vetchinin *et al.*, JETP **92**, 86 (2001).
[40] P. S. Epstein, Phys. Rev. **23**, 710 (1924).
[41] V. E. Esenkov, A. D. Usachev, and A. V. Zobnin *et al.*, in *Proceedings of Conference on Physics of Low Temperature Plasma, Part 2* (Petrozavodsk, 2004), p. 219.
[42] V. E. Fortov, A. P. Nefedov, and V. I. Molotkov *et al.*, Phys. Rev. Lett. **87**, 205002 (2001).
[43] E. S. Dzlieva, V. Yu. Karasev, and A. I. Eikhval'd, in *Proceedings of Conference on Optical Methods of Investigation of Flows* (Moscow, 2003), p. 254.
[44] E. S. Dzlieva, V. Yu. Karasev, and A. I. Eikhval'd, Opt. Spectrosc. **101**, 493 (2006).
[45] A. I. Eichvald, V. Yu. Karasev, and E. S. Dzlieva, in *Proceedings of the 5th International Conference on Plasma Physics & Plasma Technology* (Minsk, 2006), p. 392.
[46] Yu. B. Golubovsky and S. U. Nisimov, J. Tech. Phys. **40**, 24 (1995).
[47] R. A. Quinn, C. Cui, J. Goree, J. B. Pieper, H. Thomas, and G. E. Morfill, Phys. Rev. E **53**, R2049 (1996).
[48] D. G. Grier and Ch. A. Murray, J. Chem. Phys. **100**, 9088 (1994).
[49] A. Yu. Ivanov, E. S. Dzlieva, V. Yu. Karasev, and A. I. Eikhval'd, Opt. Spectrosc. (to be published).
[50] D. R. Nelson, in *Phase Transitions and Critical Phenomena*, edited by C. Domb and J. L. Leibowitz (Academic Press, London, 1983), p. 1.
[51] G. E. Morfill, H. Thomas, U. Konopka, and M. Zuzic, Phys. Plasmas **6**, 1769 (1999).
[52] H. Thomas and G. E. Morfill, Nature (London) **379**, 806 (1996).
[53] A. I. Eichvald, V. Yu. Karasev, and E. S. Dzlieva *et al.*, in *Proceedings of the 5th International Conference on Plasma Physics & Plasma Technology* (Minsk, 2006), p. 412.